Advanced Science Letters
Vol. 3, 363–367, 2010

Synthesis and Studies of $Pb_{0.76}Ca_{0.24}TiO_3$ Nanoparticles Derived by Sol–Gel

Satyendra Singh and S. B. Krupanidhi*

Materials Research Centre, Indian Institute of Science, Bangalore 560012, India

$Pb_{0.76}Ca_{0.24}TiO_3$ (PCT24) nanoparticles were synthesized by modified sol–gel method and characterized by a number of experimental techniques such as X-ray diffraction, TGA-DTA, FTIR and transmission electron microscopy equipped with energy-dispersive X-ray spectroscopy (EDX). X-ray diffraction (XRD) and selected-area electron diffraction (SAED) investigations demonstrated that the postannealed (650 °C for 1 h) PCT24 nanoparticles have tetragonal perovskite crystal structure. TEM have been employed to characterize the morphology, structure and composition of the as prepared nanoparticles. Dielectric results indicates the evidence for relaxor type behavior while observed leaky ferroelectric loops may be because of the defects such as grain boundaries and the pores in the sample as the sample was not heated at higher temperature, to retain the nanosize dimension of the particles.

1. INTRODUCTION

Ferroelectric nanostructures such as nanoparticles, nanotubes and nanowires have taken increasingly important role because of their promising applications in nanoscale piezoelectric actuators and transducers, nonvolatile memory devices, and ultrasonic devices.[1–7] A lot of research has been done on nanoferroelectric devices for memory and other applications.[8–11] Lead calcium titanate, $Pb_{1-x}Ca_xTiO_3$ (PCT) system has been widely studied due to their excellent ferroelectric, piezoelectric and pyroelectric properties.[12–14] Particularly, $Pb_{0.76}Ca_{0.24}TiO_3$ has a high piezoelectric anisotropy which is preferred than lead zirconate titanate (PZT) for some applications, like high hydrophones and high frequency use.[15–17] Furthermore, in thin film form, it has a longitudinal piezoelectric coefficient (d_{33}) almost as high as bulk, which has not been achieved in any other systems.[18,19] PCT is a solid solution between calcium titanate, $CaTiO_3$, (CT) and lead titanate, $PbTiO_3$, (PT). PT is one of the most well known ferroelectric ABO_3-type perovskite material, and has a ferroelectric tetragonal structure, while CT is an orthorhombic paraelectric material with the perovskite structure. PT shows a cubic to tetragonal phase transition at Curie point $T_c \approx 490$ °C. At room temperature, PT exhibits the largest saturation polarization ($P_s \cong 81$ $\mu C/cm^2$, as calculated theoretically) amongst all the known perovskite ferroelectrics. Its ferroelectric to paraelectric phase transition is characterized by a dielectric anomaly and drastic change in unit cell volume and tetragonal strain at the Curie point.[20,21] Ca^{2+} substitution at A site leads to a lowering in the tetragonality (c/a) ratio of the structure producing shifting to lower temperature of the ferroelectric to paraelectric transition, reducing the remnant polarization and increasing the room temperature dielectric constant.[22–24] The synthesis of ferroelectric PCT nanostructures with a controllable size and shape is critical not only in new nano-scale device application but also from a fundamental point of view. In this manuscript we report the synthesis and characterization of $Pb_{1-x}Ca_xTiO_3$ for $x = 0.24$ (PCT24) nanoparticles. PCT24 ceramic was prepared from PCT24 nanoparticles ensuring that particle size did not increase and electrical measurements were carried out.

2. EXPERIMENTAL DETAILS

The sol–gel process for synthesizing PCT24 nanoparticles is summarized in the flow chart, shown in Figure 1. Firstly, PCT24 precursor solution was prepared by a modified sol–gel method based on a previous report.[25] The metal precursors for lead, calcium and titanium were chosen depending on their reactivity and solubility in the common solvent. The precursors containing lead (Pb), calcium (Ca), titanium (Ti) were lead acetate trihydrate [$Pb(CH_3CO_2)_2 \cdot 3H_2O$), Aldrich, 99.99%], calcium acetate monohydrate [$Ca(CH_3CO_2)_2 \cdot H_2O$, Aldrich, 99.99%] and titanium (IV) isopropoxide [$Ti\{OCH(CH_3)_4\}$, Aldrich, 99.99%], (TIP), respectively. Glacial acetic acid and 2-methoxyethanol [$CH_3OC_2H_4OH$] were used as the solvent and formamide as a chemical modifier. The molar ratio among the three metal precursors was maintained as (Pb + Ca):Ti = 1:1. The PCT24 precursor solution was prepared by dissolving lead acetate trihydrate and calcium acetate monohydrate in acetic acid and 2-methoxyethanol, which was heated up to 90 °C under mild stirring until a clear solution was

*Author to whom correspondence should be addressed.

 1936-6612/2010/3/363/005 doi:10.1166/asl.2010.1136

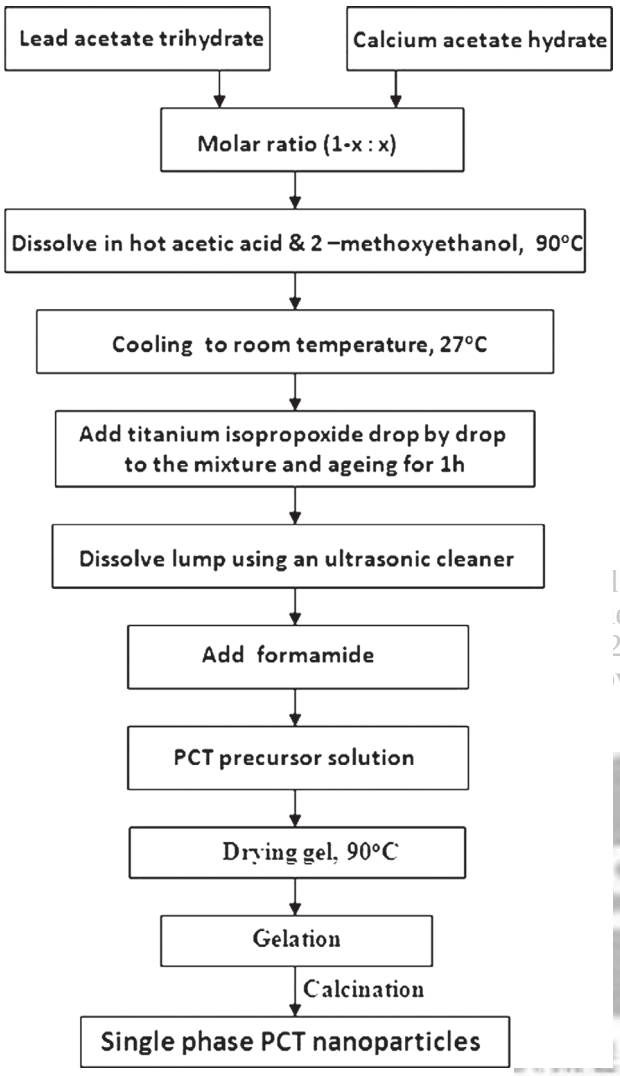

Fig. 1. Flow-chart describing the procedure for the preparation of PCT nanoparticles.

obtained. The solution was cooled to room temperature and then TIP was added drop by drop under constant stirring. Since TIP is extremely hygroscopic and has low volatility, it was added to the dehydrated solution and in a dry ambient on a clean air bench. As soon as TIP is added, an exothermic reaction is found to occur, and a part of it begins to form a lump. Hence the resulting solution is rigorously mixed at room temperature in an ultrasonic bath until the lump dissolves completely. The solution is diluted with formamide, which is a chemical modifier and enhances the stability of the solution and controls the rate of pyrolysis. The concentration of the final solution was adjusted to 0.3 M with a pH value of ∼5 by adding 2-methoxyethanol and acetic acid. The solution is finally filtered through a micro-fiber filter paper to obtain the final PCT24 precursor solution. The PCT24 precursor solution was heated on a hot plate whose temperature was increased gradually to 150 °C to evaporate the water/solvents. The sol, in turn, was heated in a furnace at 250 °C for about 2 h until a porous material was obtained as a result of complete removal of water molecules. This was grinded to fine powder and further annealed at 650 °C for 1 h by using a thermal annealing furnace to obtain the perovskite phase. Powder X-ray diffraction (XRD) pattern of the PCT24 nanoparticles powder was collected on a Philips PW3710 diffractometer (Cu-K_α radiation, 30 kV and 20 mA, $\lambda = 1.5406$ Å) from 20 to 65° at a scanning rate of 2°/min. The morphology, selected-area electron diffraction (SAED), structure and composition of the resulting PCT24 nanoparticles was examined by transmission electron microscope (TEM, Tecnai F30, equipped with EDX) with an accelerating voltage of 200 kV. For dielectric measurements, the required pellet was prepared from nanoparticles under a load of 50 kN and the pellets were then sintered at 500 °C for 2 h, the parameters ensuring that particle size did not increase. Silver paste was used to make contacts to the electrodes.

3. RESULTS AND DISCUSSION

To understand the crystallization of sol–gel derived powders, the TGA-DTA thermograms were obtained on the PCT24 precursor solution in the temperature range between 30 and 800 °C at a heating rate of 10 °C/min, shown in Figure 2. Total weight loss from 30 to 800 °C of PCT24 precursor solution was about 92.5%. The maximum weight loss of about 85% occurred from room temperature to 90 °C, which may be attributed to the evaporation of organic solvent like glacial acetic acid, 2-methoxyethanol and water. This weight loss corresponds to a sharp endothermic peak (dip in the curve due to absorbtion of heat energy) around at 82 °C in the DTA curve. About 4.7% weight loss was observed between 90 and 300 °C may be associated with the pyrolysis of propoxy and acetate ligands associated with oxide formation of metal ions. A sharp exothermic peak around at 290 °C can be attributed to the formation of pyrochlore phase. After 300 °C, no significant weight loss was observed up to 800 °C. This result gives evidence for the absence of organic residues and proves the stability of the obtained particles at high temperatures, especially regarding the commonly observed PbO loss through evaporation at higher temperatures.

Figure 3 shows FTIR spectra of the PCT24 gel powders, annealed at various temperatures, in mid-IR region (400–4000 cm^{-1}). The broad band around 3422 cm^{-1} corresponds to the (O–H) stretching vibration of hydroxyl groups of alcohols and water. The H–O–H bending mode characteristic of water

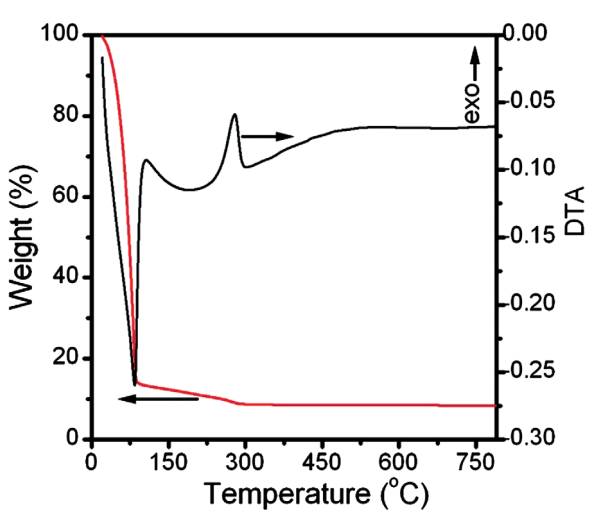

Fig. 2. TGA-DTA curves of PCT24 precursor solution.

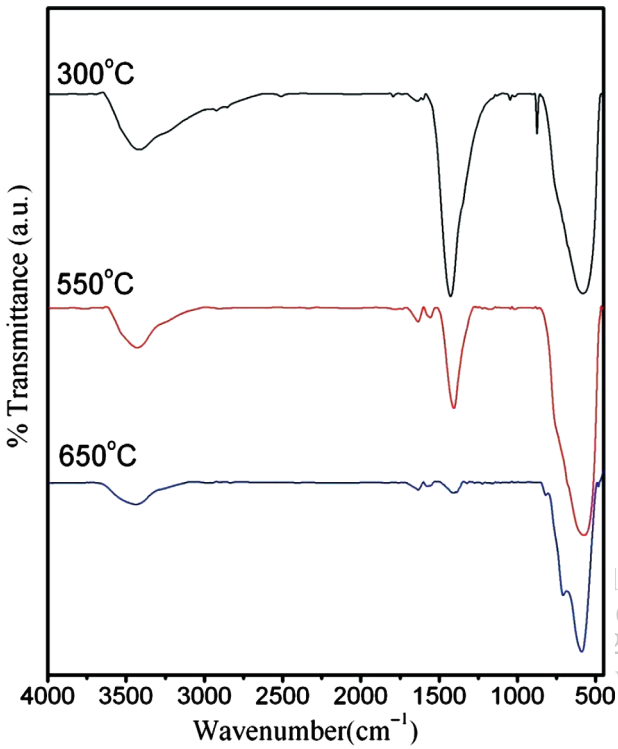

Fig. 3. FTIR spectra of PCT24 gel powder annealed at different temperatures.

appears at 1635 cm^{-1}. The peaks at 1408 and 1555 cm^{-1} may be ascribed to ν_{sym} (COO$^-$) and ν_{asym} (COO$^-$) of acetyl groups, respectively. The small peaks around 1047 cm^{-1} may be the C–H rocking modes. The broad band in the low wavenumber range (at about 580 cm^{-1}) is attributed to the Ti–O bonds, which comes from the envelope of the photon bands of a metal-oxygen-metal bond of a solid oxide network. With increasing calcination temperature, the intensities of 1408 and 1635 cm^{-1} drastically decreased, and the C–H rocking modes at 1047 cm^{-1} completely disappeared. In addition, no COO$^-$ vibrations were observed indicating complete removal of organics. These observations suggest that PCT crystallizes at an annealing temperature of 650 °C. These results are qualitatively similar to those of Bao et al.[26]

Figure 4 shows the XRD pattern of the PCT24 nanoparticles powder after annealing at 650 °C for 1h at room temperature. It is evident from XRD pattern that as prepared PCT24 nanoparticles are crystalline and no secondary phases were observed. All the diffraction peaks could be indexed and matched well with the tetragonal perovskite phase of PCT bulk (JCPDS No 04-002-9067). The average crystallite size was found to be about 48.6 nm for the sample annealed at 650 °C, which was calculated from Scherrer's formula by indexing (101) peak as follows; $T = 0.9\lambda/\beta\cos\theta_B$, where T is the average particle size in angstroms, β is the FWHM (full width of half maximum) in radians, λ (=1.5406 Å) is the wavelength in angstroms, and θ_B is the Bragg angle in degrees.

Figure 5(a) shows the TEM image of the as-prepared PCT24 nanoparticles. The micrograph clearly shows that the particles are in the range of 30–55 nm. Figure 5(b) shows the selected area electron diffraction (SAED) pattern taken on a PCT24 nanoparticle, indicates the single crystalline nature. The

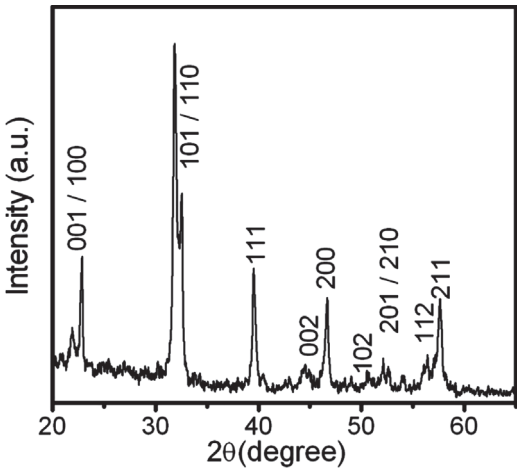

Fig. 4. XRD pattern of PCT24 nano-powder annealed at 650 °C.

microstructure of the PCT24 nanoparticles was further investigated using high resolution TEM (HRTEM). Figure 5(c) shows the HRTEM image taken on a single PCT24 nanoparticle, which gives further insight into the details of the structure. The distance between the parallel fringes to be about 2.81Å, corresponding to the well-recognized d-spacing of {101} atomic plane, which agrees well with the values, calculated from the SAED pattern and open literature (JCPDS No 04-002-9067). In order to confirm the chemical composition of PCT24 nanoparticles, EDX spectroscopy was taken at a number of nanoparticles by the TEM. Figure 5(d) shows the EDX spectrum from a PCT24 nanoparticle. It is clear from EDX spectrum that these nanoparticles are composed of the Pb, Ca and Ti atoms. The atomic ratio of Pb, Ca and Ti was around 0.755:0.245:0.992, which is very close to the

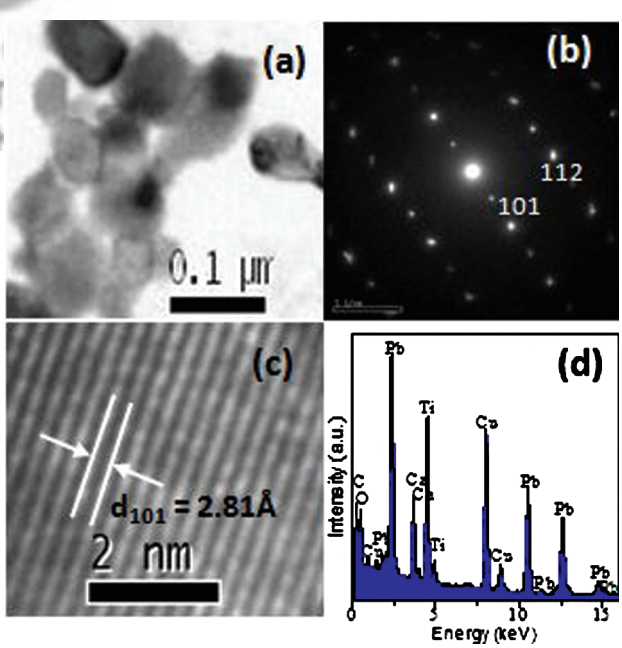

Fig. 5. TEM images: (a) PCT24 nanoparticles annealed at 650 °C, (b) Electron diffraction pattern taken on a PCT24 nanoparticle showing single crystalline nature, (c) HRTEM image of a single PCT24 nanoparticle, and (d) EDX spectrum from a single PCT24 nanoparticle.

nominal composition $Pb_{0.76}Ca_{0.24}TiO_3$. No emission lines from other elements were present in the spectrum, thereby confirming the absence of any impurities from reactants. The presence of the Cu peaks may be attributed to the Cu present in the grid.

It is well known that $Pb_{1-x}Ca_xTiO_3$ bulk materials show ferroelectric properties up to $x = 0.4$.[27] Ranjan et al.[28] have reported an orthorhombic distortion ($x > 0.42$) and relaxor behavior at $x = 0.5$. It is well-known that ferroelectric bulk materials with the perovskite structure for example, lead titanate shows a sharp phase transition at the Curie temperature T_C (490 °C) and almost no frequency dependence of the temperature curve of the dielectric constant up to the GHz frequency region. Above T_C the temperature dependence of the dielectric constant follows the Curie-Weiss law [Eq. (1) with $\gamma = 1$];

$$\frac{1}{\varepsilon} - \frac{1}{\varepsilon_m} = \frac{1}{C}(T - T_C)^{\gamma} \quad (1)$$

where ε_m is the maximum value of dielectric constant, C is the Curie-Weiss-like constant and γ is the critical exponent. Relaxors are closely related to ferroelectrics and shows a diffuse phase transition and a large frequency dependence of the much broader temperature curve of the dielectric constant. The broad temperature dependence of the dielectric constant of the relaxors obeys a modified Curie-Weiss law [Eq. (1) with $\gamma \approx 2$ and $T_c = T_m$].[29] The temperature T_m is no longer a phase transition temperature but marks the temperature of the maximum dielectric constant. The temperature T_m is moving to higher values with increasing measurement frequency and the maximum value is being reduced. This pronounced frequency dependence is produced by a broad relaxation time spectrum.

Figure 6 shows the variation of the real part of the dielectric constant of a PCT24 ceramic prepared from nanoparticles as a function of temperature at few selected frequencies. It is interesting to note that for all frequencies, the curves were broadened which indicates a diffuse phase transition. In addition, they show frequency dependence of T_m (the temperature at which dielectric constant show maxima) from 281 °C at 1 kHz to 290 °C at 1 MHz as can be seen from Figure 6. This proves that T_m shifts to higher temperatures with increasing measurement frequency. From a plot of $\ln(1/\varepsilon - 1/\varepsilon_m)$ versus $\ln(T - T_m)$ in the paraelectric region, shown in the inset of Figure 6, one obtains an exponent of $\gamma \approx 1.81$. These dielectric results clearly indicate that PCT24 ceramic prepared from nanoparticles gives the evidence for relaxor type behavior. One can say that the grain size is playing a vital role for this type of behavior. The same behavior was observed by Ziebert et al.[30] in nanocrystalline thin film of PCT for the same composition. Polarization versus electric field (P vs. E) hysteresis behavior was studied using a modified Sawyer-Tower circuit. Figure 7 shows the room temperature P–E hysteresis loops of the ceramic prepared from nanoparticles measured at different applied voltages at 1 kHz frequency. It is evident from figure that the observed ferroelectric loops are leaky in nature. The reason for the leaky loop may be because of the defects such as grain boundaries and the pores in the sample as the sample was not heated at higher temperature, to retain the one dimension of the particles.

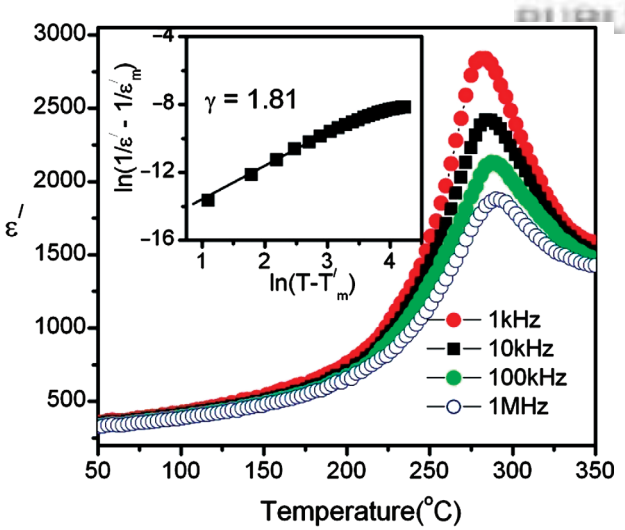

Fig. 6. Frequency dependence of the temperature curves of the real part of the dielectric constant (ε') of a PCT24 ceramic prepared from nanoparticles and the inset shows the $\ln(1/\varepsilon - 1/\varepsilon_m)$ versus $\ln(T - T_m)$ plot in the paraelectric region.

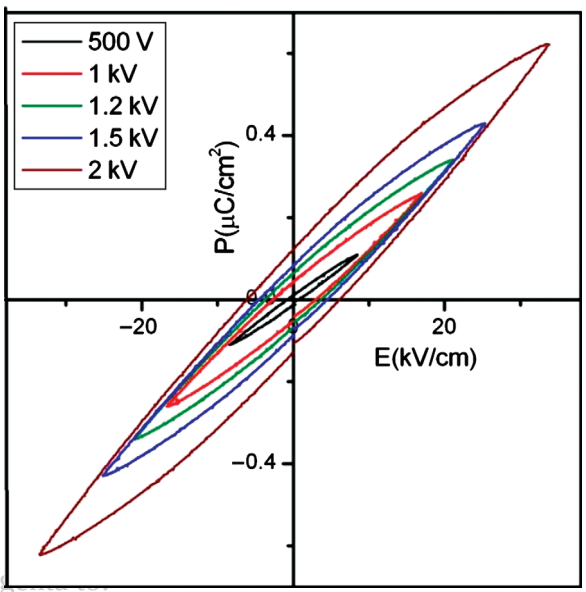

Fig. 7. Room temperature P–E hysteresis loops for the PCT24 ceramic prepared from nanoparticles measured at different applied voltages.

4. CONCLUSIONS

In summary, PCT24 nanoparticles were synthesized by modified sol–gel method and characterized by number of techniques. Dielectric results indicate that PCT24 ceramic prepared from nanoparticles gives the evidence for relaxor type behavior. Leaky ferroelectric loops were observed may be because of the defects such as grain boundaries and the pores in the sample as the sample was not heated at higher temperature, to retain the one dimension of the particles.

References and Notes

1. H. Ahn, K. M. Rabe, and J. M. Triscone, *Science* 303, 488 **(2004)**.
2. J. Junquera and P. Ghosez, *Nature* 422, 506 **(2003)**.
3. Y. Wang and J. J. Santiago-Aviles, *Nanotechnology* 15, 32 **(2004)**.

4. Y. Luo, I. Szafraniak, N. D. Zakharov, V. Nagarajan, M. Steinhart, R. B. Wehrspohn, J. H. Wendorff, R. Ramesh, and M. Alexe, *Appl. Phys. Lett.* 83, 440 **(2003)**.
5. M. W. Chu, I. Szafraniak, R. Scholz, C. Harnagea, D. Hesse, M. Alexe, and U. Gosele, *Nat. Mater.* 3, 87 **(2004)**.
6. A. Roelofs, I. Schneller, K. Szot, and R. Waser, *Appl. Phys. Lett.* 81, 5231 **(2002)**.
7. J. F. Scott and C. A. P. de Araujo, *Science* 246, 1400 **(1989)**.
8. J. F. Scott, M. Alexe, N. D. Zakharov, A. Pignolet, C. Curran, and D. Hesse, *Integr. Ferroelectr.* 21, 1 **(1998)**.
9. J. F. Scott, *Ferroelectrics* 314, 207 **(2005)**.
10. A. Gruverman and A. Kholkin, *Rep. Prog. Phys.* 69, 2443 **(2006)**.
11. J. F. Scott, F. D. Morrison, M. Miyake, and P. Zubko, *Ferroelectrics* 336, 237 **(2006)**.
12. H. Y. Guo, J. B. Xu, Z. Xie, E. Z. Zuo, I. H. Wilson, and W. L. Zhong, *Solid State Commun.* 121, 603 **(2002)**.
13. H. Y. Guo, J. B. Xu, I. H.Wilson, Z. Xie, and E. Z. Luo, *Phys. Lett. A* 294, 217 **(2002)**.
14. F. M. Pontes, D. S. L. Pontes, E. R. Leite, E. Longo, E. M. S. Santos, S. Mergulhao, A. Chiquito, P. S. Pizani, F. Lanciotti, Jr., T. M. Boschi, and J. A. Varela, *J. Appl. Phys.* 91, 6650 **(2002)**.
15. Y. Yamashita, K. Yokogama, H. Honda, and T. Takahashi, *Jpn. J. Appl. Phys.* 20, 183 **(1981)**. Suppl. 20–24.
16. K. M. Rittenmyer and R. Y. Ting, *Ferroelectrics* 110, 171 **(1990)**.
17. K. Uchino and K. Y. Oh, *J. Am. Ceram. Soc.* 74, 1131 **(1991)**.
18. A. Kholkin, A. Seifert, and N. Setter, *App. Phy. Lett.* 72, 3374 **(1998)**.
19. A. L. Kholkin, M. L. Calzada, P. Ramos, J. Mendiola, and N. Setter, *Appl. Phys. Lett.* 69, 3602 **(1996)**.
20. G. Shirane, S. Hoshino, and K. Suzuki, *Phys. Rev.* 80, 1105 **(1950)**.
21. N. Takesue and H. Chen, *J. Appl. Phys.* 76, 5856 **(1994)**.
22. E. Sawaguchi and M. L. Charters, *J. Am. Ceram. Soc.* 42, 157 **(1959)**.
23. E. Sawaguchi, T. Mitsuma, and Z. Ishii, *J. Phys. Soc. Jap.* 11, 1298 **(1956)**.
24. J. Mendiola, B. Jimenez, C. Alemany, L. Pardo, and L. Del Olmo, *Ferroelectrics* 94, 183 **(1989)**.
25. A. K. S. Chauhan, V. Gupta, and K. Sreenivas, *Mater. Sci. Eng., B* 130, 81 **(2006)**.
26. D. Bao, X. Wu, L. Zhang, and X. Yao, *Thin Solid Films* 350, 33 **(1999)**.
27. E. Sawaguchi and M. L. Charters, *J. Am. Chem. Soc.* 42, 157 **(1959)**.
28. R. Ranjan, N. Singh, D. Pandey, V. Siruguri, P. S. R. Krishna, S. K. Paranjpe, and A. Banerjee, *Appl. Phys. Lett.* 70, 3221 **(1997)**.
29. B. Kirsch, H. Schmitt, and H. Müser, *Ferroelectrics* 68, 275 **(1986)**.
30. C. Ziebert, H. Schmitt, J. K. Krüger, A. Sternberg, and K.-H. Ehses, *Phys. Rev. B* 69, 214106 **(2004)**.

Received: 10 August 2009. Accepted: 30 January 2010.